Biogeochemical context impacts seawater pH changes resulting from atmospheric sulfur and nitrogen deposition

Mathilde Hagens,[1] Keith A. Hunter,[2] Peter S. Liss,[3,4] and Jack J. Middelburg[1]

[1]Department of Earth Sciences – Geochemistry, Utrecht University, Utrecht, The Netherlands.

[2]Division of Sciences, University of Otago, Dunedin, New Zealand.

[3]School of Environmental Sciences, University of East Anglia, Norwich, UK.

[4]Department of Oceanography, Texas A & M University, College Station, TX, USA.

Corresponding author:

M. Hagens, Department of Earth Sciences – Geochemistry, Utrecht University, P.O. Box 80.021, 3508 TA Utrecht, The Netherlands. (m.hagens@uu.nl)

This article has been accepted for publication and undergone full peer review but has not been through the copyediting, typesetting, pagination and proofreading process which may lead to differences between this version and the Version of Record. Please cite this article as doi: 10.1002/2013GL058796

Abstract

Seawater acidification can be induced both by absorption of atmospheric carbon dioxide (CO_2) and by atmospheric deposition of sulfur and nitrogen oxides and ammonia. Their relative significance, interplay and dependency on water-column biogeochemistry are not well understood. Using a simple biogeochemical model we show that the initial conditions of coastal systems are not only relevant for CO_2-induced acidification, but also for additional acidification due to atmospheric acid deposition. Coastal areas undersaturated with respect to CO_2 are most vulnerable to CO_2-induced acidification, but are relatively least affected by additional atmospheric deposition-induced acidification. In contrast, the pH of CO_2-supersaturated systems is most sensitive to atmospheric deposition. The projected increment in atmospheric CO_2 by 2100 will increase the sensitivity of coastal systems to atmospheric deposition-induced acidification by up to a factor 4, but the additional annual change in proton concentration is at most 28%.

1. Introduction

Combustion of biomass and fossil fuels releases SO_x and NO_x to the atmosphere. Due to the short (i.e., ~1 week) residence time of atmospheric sulfur (S) and nitrogen (N) oxides, their deposition in the marine realm occurs mainly in coastal areas downwind of the principal terrestrial source regions [*Rodhe et al.*, 2002] and in waters with intensive shipping [*Tsyro and Berge*, 1997]. In marine systems, atmospheric S and N oxides eventually end up as H_2SO_4 and HNO_3, either through chemical alterations in the atmosphere and wet deposition of H_2SO_4 and HNO_3, or through dry deposition of SO_x and NO_x and subsequent fast hydration in the seawater [*Doney et al.*, 2007]. Absorption of S and N oxides by seawater thus causes a decrease in total alkalinity (TA) and hence a lowering in pH, whereby the effect of S oxide deposition on TA is twice as high as the effect of N oxide deposition [*Doney et al.*, 2007; *Hunter et al.*, 2011].

Ammonia (NH_3) emissions originate mostly from animal husbandry and fertilizer use and its deposition to marine systems causes an increase in TA and hence a rise in pH. However, in the atmosphere NH_3 can be transformed to acidic N through various processes [*Dentener and Crutzen*, 1994] and when any of the deposited NH_3 is nitrified, the alkaline flux effectively changes to an acidity flux with the same stoichiometry as N oxide deposition [*Doney et al.*, 2007; *Hunter et al.*, 2011].

While acidification of terrestrial and freshwater systems due to atmospheric deposition has been investigated for decades [*Schindler*, 1988], there are very few studies explicitly dealing with the effects of atmospheric deposition on seawater pH. Seawater acidification induced by absorption of CO_2 and by atmospheric deposition co-occur, but their relative importance and interactions (synergistic or antagonistic) have been poorly documented. Using time series of rainfall and seawater CO_2

parameters in the North Atlantic Ocean near Bermuda, *Bates and Peters* [2007] showed that wet deposition of acids contributes at most 2-5% to surface water acidification. By coupling a biogeochemical model to a global circulation model, *Doney et al.* [2007] found a similar magnitude of the contribution of anthropogenic S and N deposition to surface water acidification, but they calculated changes in carbonate chemistry as high as 10-50% of the CO_2-induced changes close to source regions and in shallow seas. *Hunter et al.* [2011] focused on three coastal seas and reported that atmospheric inputs of strong acids compensate the CO_2-induced acidification. This implies that ocean acidification trajectories based on CO_2 absorption alone provide an incomplete, biased picture. *Hassellöv et al.* [2013] focused on global acidification due to shipping activities and found that in certain coastal hotspots shipping-based acidification can be of the same order of magnitude as CO_2-induced acidification.

Although the three modeling studies [*Doney et al.*, 2007; *Hunter et al.*, 2011; *Hassellöv et al.*, 2013] used a similar approach, their estimated contribution of atmospheric deposition to ocean acidification varies from negligible to substantial. This is due to differences in the systems and processes considered, and in the way the effects of atmospheric S and N deposition on seawater pH are quantified. Here we use a simple model to identify key factors and to explain the effect of different initial conditions on the additive pH change due to atmospheric acid deposition.

2. Methodological considerations

2.1. The fraction of atmospheric NH_3 deposition that will be nitrified

The fraction of deposited NH_3 that is nitrified is highly relevant for the calculated changes in TA and pH [*Doney et al.*, 2007; *Hunter et al.*, 2011]. Because

this fraction is poorly known, likely variable, and timescale-dependent, these studies considered the two extreme cases (i.e., zero and complete nitrification of the deposited NH_3). Including biological feedbacks due to enhanced N availability, which may especially be of importance in N-limited coastal marine ecosystems, *Doney et al.* [2007] found that globally ca. 98% of the deposited NH_3 will be nitrified over a time span of 10 years.

For studies focusing on the seasonal to interannual scales, we propose to use the parameterization by *Yool et al.* [2007] who, based on a compilation of a global data set, suggested a mean specific nitrification rate of 0.2 d^{-1}. If we include their lower (0.02 d^{-1}) and upper (2 d^{-1}) limits and convert to percentages of ammonia being used for nitrification, this leads to values of 43, 16 and 81%, respectively, of which the lower estimate is close to the 15% suggested by *Middelburg and Soetaert* [2004] for the North Sea.

2.2. Open versus closed system calculations

So far, modeling studies have adopted different strategies to calculate the effect of atmospheric deposition on seawater pCO_2 ($pCO_{2,sw}$) and thus acidification:

1. *Hunter et al.* [2011], in four of their scenarios ("CO_2+SO_x", "CO_2+SO_x+NO_x", "CO_2+SO_x+NO_x+NH_3" and "After nitrification"), and *Hassellöv et al.* [2013] did not allow re-equilibration of $pCO_{2,sw}$ with the atmosphere (closed system).
2. In their "after buffering" scenarios *Hunter et al.* [2011] restored $pCO_{2,sw}$ values to their original values, i.e., full re-equilibration of $pCO_{2,sw}$ with the atmosphere (open system).
3. *Doney et al.* [2007] dynamically calculated $pCO_{2,sw}$ values at each time step taking CO_2 equilibration and atmospheric deposition into account.

The first approach neglects air-sea exchange of CO_2, is limited to the additive effect of atmospheric CO_2 uptake and acid deposition and results in too much acidification. The second approach restores $pCO_{2,sw}$ values and in this way numerically generates CO_2 effluxes that modulate the decrease in pH. The third approach, in contrast, allows for simultaneous calculation of all processes, thus producing the most accurate $pCO_{2,sw}$ values. However, the choice for a specific approach highly depends on the time scale of the study. *Doney et al.* [2007] looked at annual changes in a time span of 10 years using small time steps, highlighting the need for an iteratively determined $pCO_{2,sw}$. *Hunter et al.* [2011] considered 1 year, an interval in which $pCO_{2,sw}$ may be assumed to be in equilibrium with atmospheric pCO_2 ($pCO_{2,atm}$). However, *Hassellöv et al.* [2013] used monthly intervals over a 1-year period where $pCO_{2,sw}$ was updated using measured rather than calculated data. This approach led to an overestimation of the calculated total surface water acidification in CO_2-supersaturated systems.

2.3. Supersaturated versus undersaturated systems

In natural systems, $pCO_{2,sw}$ can be out of equilibrium with $pCO_{2,atm}$ [*Takahashi et al.*, 2009], either seasonally due to biological activity and/or temperature effects, or more permanently as a result of their hydrodynamic setting. The time scale at which $pCO_{2,sw}$ equilibrates with the atmosphere (~weeks) is long compared to the residence time of atmospheric S and N oxides (~days), indicating the potential for atmospheric deposition to influence the equilibration process. The decrease in TA caused by atmospheric S and N deposition and associated increase in $pCO_{2,sw}$ will have different effects on CO_2-supersaturated and undersaturated systems. The direction and rate of CO_2 air-sea exchange are thus key to accurate projection of seawater acidification. We illustrate this with a simple case study.

A comparison is made of three systems which have the same TA, salinity and temperature but differ in their initial $pCO_{2,sw}$. System one is initially in equilibrium with $pCO_{2,atm}$. In the second, undersaturated system 11.5 μmol kg^{-1} yr^{-1} of dissolved inorganic carbon (DIC) is removed by biological processes, resulting in an initial $pCO_{2,sw}$ of 250 ppmv. The third, supersaturated system has an initial $pCO_{2,sw}$ of 600 ppmv, corresponding to a net DIC production of 17.4 μmol kg^{-1} yr^{-1}. Using a time step of 1 year, we calculated the net effect on $pCO_{2,sw}$ and pH of: (1) a constant acid deposition flux where either zero or complete nitrification of the deposited NH_3 results in a TA decrease of 1.34 and 3.94 μmol kg^{-1} yr^{-1}, respectively; and (2) increasing $pCO_{2,atm}$ to 936 ppmv in 2100 according to the output of the RCP8.5 scenario [*Meinshausen et al.*, 2011]. Air-sea exchange of CO_2 was calculated using a simple kinetic rate law

$$R = k\left(CO_2^{sat} - [CO_2]\right) \quad (1)$$

with a rate constant k of 2 yr^{-1}, so that there was incomplete equilibration with the atmosphere.

All three systems show an increase in $pCO_{2,sw}$ and a decrease in pH (Figure 1). Atmospheric deposition causes further decreases in pH, because the additional lowering in TA reduces the capacity of the system to buffer changes. Consistent with *Doney et al.* [2007] and *Hunter et al.* [2011], nitrification of atmospheric NH_3 leads to lower pH values.

The sensitivity towards ocean acidification and the interaction with atmospheric deposition depend on the biogeochemical context, i.e., the biological (or physical) processes adding or removing DIC, moderated by CO_2 air-sea exchange. The undersaturated system is most sensitive to CO_2-induced acidification (ΔpH is -0.431), as the enhanced gradient between $pCO_{2,atm}$ and $pCO_{2,sw}$ increases the CO_2

influx. Atmospheric deposition, however, lowers this CO_2 gradient, resulting in a reduced influx. As a result, this system is relatively least vulnerable to atmospheric deposition (additional decrease in proton concentration ($[H^+]$) of 11.5% and 38.0% excluding and including nitrification, respectively). The reverse holds for the supersaturated system, where the CO_2-induced ΔpH is -0.255. Here, a higher $pCO_{2,sw}$ resulting from atmospheric deposition increases the gradient between $pCO_{2,sw}$ and $pCO_{2,atm}$ and thus leads to a higher CO_2 efflux, i.e., it is more perturbed. This results in a relatively higher additive $[H^+]$ decrease of 14.4% and 47.8% excluding and including nitrification, respectively.

2.4. Model description

Based on the discussion above, we extended the model of *Hunter et al.* [2011]. Rather than assuming two extreme scenarios for nitrification and outgassing of CO_2 to the atmosphere (zero versus complete), we implemented kinetic descriptions for both processes: the *Yool et al.* [2007] parameterization for nitrification (section 2.1) and a simple air-sea exchange expression

$$R_{exch} = k_d\left(CO_2^{sat} - [CO_2]\right) \quad (2)$$

with a transfer velocity k_d of 2.7 m d^{-1}, which corresponds to a wind speed of 7.6 m s^{-1} [*Liss and Merlivat*, 1986], within the range of median wind speeds for the European coastal zone [*Gazeau et al.*, 2004]. The model was run until the end of the 21st century assuming that atmospheric deposition fluxes remain constant within this time period and the increase in $pCO_{2,atm}$ follows the RCP8.5 scenario. Horizontal advection and exchanges with the deep water were not taken into account. Finally, in addition to the southern North Sea, Baltic Sea and South China Sea case studies presented by *Hunter*

et al. [2011], we included the northwestern (NW) Mediterranean Sea as a fourth case study (for parameterization see table S1 of the auxiliary material[1]).

We calculated the evolution of pH using the explicit pH modeling approach of *Hofmann et al.* [2010b] (see auxiliary materials for extensive explanation[1]). Briefly, the main advantage of this approach is that changes in pH can be directly attributed to the different processes affecting pH:

$$\frac{d[H^+]_p}{dt} = S_p R_p \tag{3}$$

Here, R_p is the rate of a process p (mol kg^{-1} yr^{-1}) and sensitivity (S_p) is defined as the ratio of a stoichiometric coefficient for the proton in the reaction (ν_H^p) and a buffer factor (β):

$$S_p = \frac{\nu_{H^+}^p}{\beta} \tag{4}$$

The buffer factor is defined as:

$$\beta = -\left(\frac{\partial TA}{\partial [H^+]}\right) \tag{5}$$

This way, all processes affecting pH can be included simultaneously while their individual contribution can still be extracted. All calculations were performed on the total pH scale using the R package *AquaEnv* [*Hofmann et al.*, 2010a] with a time step of 1 year, using the equilibrium constants of *Mehrbach et al.* [1973] as refitted by *Dickson and Millero* [1987] for the carbonate system and of *Dickson* [1990] for sulfate.

[1] Auxiliary materials are available in the HTML

3. Results

With 43% of the atmospheric NH_3 being nitrified ΔpH is smallest (-0.336) in the NW Mediterranean Sea and largest (-0.386) in the southern North Sea (Figure 2a). The latter coastal system is also most sensitive to changes in the fraction of atmospheric NH_3 deposition that is nitrified. With 16% nitrification the total pH decrease for the North Sea is 0.0128 smaller, while pH decreases by an additional 0.0187 with a fraction of 81%. For the South China Sea these numbers are slightly lower, while for the other two seas varying the degree of nitrification leads to a negligible change in the total acidification (data not shown). Comparing our results with model runs with CO_2-induced acidification only (Figure 2b), we see that the additive ΔpH due to atmospheric acid deposition is also highest (0.0430 until 2100) in the southern North Sea. The contribution of acid deposition is smallest in the NW Mediterranean Sea (0.0006 additional pH decrease until 2100), probably due to its deep mixed layer and high buffering capacity (Figure 2f).

The contribution of the processes involved in proton cycling to the net change in $[H^+]$ is shown for the southern North Sea in Figure 2c. The net change (gray line) increases with time until 2071, after which it slows down. The magnitude of $[H^+]$ change induced by each process increases with time. Atmospheric acid deposition rates are constant, so the increase in $d[H^+]/dt$ with time can be attributed directly to increased sensitivity (S_p). Air-sea exchange of CO_2 (R_{exch}), however, does not remain constant (Figure 2e) since both atmospheric and seawater CO_2 change with time. This explains why the relative contribution of CO_2 air-sea exchange to acid deposition first decreases and then increases with time (Figure 2c), following the trend in R_{exch} (Figure 2e). However, the absolute value of $[H^+]$ change is primarily controlled by the increase of S_{exch} (Figure 2d) rather than changes in R_{exch}.

Using CO_2 air-sea exchange as an example, we show that changes in sensitivity predominantly result from changes in the buffering capacity. The stoichiometric coefficient for the proton ν_H^{exch} decreases slightly until 2100, ranging from 3.9% in the Baltic Sea to 5.8% in the South China Sea (Figure 2d). Changes in the stoichiometric coefficient for the proton of nitrification (ν_H^{nitr}) are even smaller because the equilibrium constant of the NH_4^+ / NH_3 acid-base pair is far from the range of pH considered here. The buffer factor β decreases by 57% in the Baltic Sea and roughly fourfold in the southern North Sea (Figure 2f). The fourfold decrease in buffering (β) by the end of the 21st century combined with minor changes in stoichiometric coefficients for the proton (ν_H^p) means that the southern North Sea becomes about four times more sensitive to any process involving proton transfer. Differences in buffering capacity also explain why the Baltic Sea is the most sensitive and the South China Sea and NW Mediterranean Sea least sensitive to processes consuming or producing protons, as β is inversely related to S_p (equation (5)).

Increasing $pCO_{2,atm}$ is by far the most important process contributing to the total change in pH (Figure 2b), but this does not imply that CO_2 air-sea exchange dominates proton cycling (Figure 2c). The cumulative effect of atmospheric deposition is a production of protons (Figure 2c), inducing an increase of $pCO_{2,sw}$. However, at the same time the increment in $pCO_{2,atm}$ lowers the air-sea gradient of CO_2. The balance between both processes determines whether the net CO_2 flux is in or out. In the southern North Sea, the increase of $pCO_{2,sw}$ by acid deposition is stronger than the increase of $pCO_{2,atm}$, resulting in an efflux and implying proton consumption due to CO_2 air-sea exchange (negative R_{exch}, Figure 2e). Thus, the acidifying effect of a growing $pCO_{2,atm}$ is here masked in the proton balance. In the

other three seas, the increment of $pCO_{2,atm}$ dominates, resulting in net proton production (positive R_{exch}; Figure 2e).

4. Discussion

4.1. Comparison with previous studies

The global annual mean (0.00037) and median (0.00018) decrease in pH due to total atmospheric acid inputs as calculated by *Hassellöv et al.* [2013] are an order of magnitude smaller than the measured annual open-ocean acidification [*Santana-Casiano et al.*, 2007; *Midorikawa et al.*, 2012]. With the RCP8.5 scenario for $pCO_{2,atm}$, pH at our four coastal sites is expected to decrease at a magnitude roughly similar to global estimates [*Bopp et al.*, 2013]. The inclusion of atmospheric acid deposition leads to an additional change in $[H^+]$ of at most 28%, which appears to be higher than the average global contribution. However, annual acidification at two distinct coastal sites, i.e., the southern North Sea [*Provoost et al.*, 2010] and Tatoosh Island, Washington state, USA [*Wootton and Pfister*, 2012], currently occurs at a rate one order of magnitude higher than in the open ocean. This is an indication that some important processes that affect pH in coastal areas are not included in our model. Possible mechanisms are site-specific and may include alkalinity inputs from shelf sediments [*Thomas et al.*, 2009], increased upwelling [*Feely et al.*, 2008], increased inputs of riverine dissolved organic carbon [*Wootton and Pfister*, 2012] and changes in the production-respiration balance [*Borges and Gypens*, 2010; *Provoost et al.*, 2010].

4.2. Regional and saturation state-related differences

Regionally distinct initial conditions are known to influence the response of a system to increasing $pCO_{2,atm}$. For example, the Arctic Ocean is widely recognized to be one of the systems most vulnerable to increasing $pCO_{2,atm}$, because of its naturally low pH, buffering capacity and temperature [*Orr et al.*, 2005], while low-latitudinal regions are generally less susceptible to CO_2 invasion [*Egleston et al.*, 2010]. This is the first study showing that initial conditions also play a role in the effect of atmospheric acid deposition on pH.

Systems supersaturated with respect to $pCO_{2,atm}$, such as heterotrophic ecosystems where respiration exceeds gross production, are most sensitive to additive acidification by acid deposition, whereas CO_2-undersaturated systems, in particular autotrophic ecosystems, are least sensitive. The metabolic balance and CO_2 saturation conditions of coastal ecosystems are spatially and temporally heterogeneous and their role as a source or sink of atmospheric CO_2 is debated [*Cai et al.*, 2006; *Chen and Borges*, 2009]. The southern North Sea and northern part of the South China Sea are reported to be sources of CO_2 to the atmosphere [*Thomas et al.*, 2004; *Zhai et al.*, 2005]. Thus, atmospheric acid deposition strengthens the outgassing fluxes from these seas. In contrast, both the northwestern Mediterranean Sea [*Durrieu de Madron et al.*, 2003] and the Baltic Sea [*Thomas et al.*, 2010] are generally sinks of atmospheric CO_2, and atmospheric acid deposition leads to a weakened CO_2 uptake in these seas.

The spatial and temporal variability in coastal air-sea CO_2 gradients, which ranges, e.g., from ca. -100 to 100 ppmv in the southern North Sea [*Thomas et al.*, 2004], introduces uncertainty to our calculated annual CO_2 air-sea gas exchange rates. Additionally, selecting one from the several parameterizations that exist for k_d adds a factor of 2 uncertainty [*Garbe et al.*, 2014].

4.3. Future projections

Globally, atmospheric S and N emissions are expected to decline within the next century due to air-quality regulations and reduced fertilizer and fossil fuel use. However, emissions tend to become relatively more concentrated in economic growth regions such as China, India and Brazil [*Van Vuuren et al.*, 2011]. Generally speaking, low-latitudinal shelf seas and near-shore coastal areas are CO_2-supersaturated, while CO_2-undersaturated shelf seas are mostly found at mid- to high-latitudes [*Chen and Borges*, 2009]. Since most economic growth regions are present at low latitudes, their CO_2-supersaturated coastal systems are especially vulnerable to future acid deposition.

5. Acknowledgements

This research is supported by a Sea and Coastal Research fund (83910502) of the Netherlands Organisation for Scientific Research (NWO). The idea for this paper came from the deliberations of GESAMP Working Group 38, the Atmospheric Input of Chemicals to the Ocean. We thank both reviewers for their constructive comments that have significantly improved the paper.

6. References

Bates, N. R., and A. J. Peters (2007), The contribution of atmospheric acid deposition to ocean acidification in the subtropical North Atlantic Ocean, *Mar. Chem.*, *107*(4), 547–558, doi:10.1016/j.marchem.2007.08.002.

Bopp, L. et al. (2013), Multiple stressors of ocean ecosystems in the 21st century: projections with CMIP5 models, *Biogeosciences*, *10*, 6225–6245, doi:10.5194/bg-10-6225-2013.

Borges, A. V., and N. Gypens (2010), Carbonate chemistry in the coastal zone responds more strongly to eutrophication than ocean acidification, *Limnol. Oceanogr.*, *55*(1), 346–353, doi:10.4319/lo.2010.55.1.0346.

Cai, W.-J., M. Dai, and Y. Wang (2006), Air-sea exchange of carbon dioxide in ocean margins: A province-based synthesis, *Geophys. Res. Lett.*, *33*(12), L12603, doi:10.1029/2006GL026219.

Chen, C.-T. A., and A. V. Borges (2009), Reconciling opposing views on carbon cycling in the coastal ocean: Continental shelves as sinks and near-shore ecosystems as sources of atmospheric CO_2, *Deep Sea Res. Part II Top. Stud. Oceanogr.*, *56*(8-10), 578–590, doi:10.1016/j.dsr2.2009.01.001.

Dentener, F., and P. Crutzen (1994), A three-dimensional model of the global ammonia cycle, *J. Atmos. Chem.*, *19*, 331–369, doi:10.1007/BF00694492.

Dickson, A. G. (1990), Standard potential of the reaction: $AgCl(s) + ½H_2(g) = Ag(s) + HCl(aq)$, and the standard acidity constant of the ion HSO_4^- in synthetic sea water from 273.15 to 318.15 K, *J. Chem. Thermodyn.*, *22*(2), 113–127, doi:10.1016/0021-9614(90)90074-Z.

Dickson, A. G., and F. J. Millero (1987), A comparison of the equilibrium constants for the dissociation of carbonic acid in seawater media, *Deep Sea Res. Part A. Oceanogr. Res. Pap.*, *34*(10), 1733–1743, doi:10.1016/0198-0149(87)90021-5.

Doney, S. C., N. Mahowald, I. Lima, R. A. Feely, F. T. Mackenzie, J.-F. Lamarque, and P. J. Rasch (2007), Impact of anthropogenic atmospheric nitrogen and sulfur deposition on ocean acidification and the inorganic carbon system, *Proc. Natl. Acad. Sci. U. S. A.*, *104*(37), 14580–14585, doi:10.1073/pnas.0702218104.

Durrieu de Madron, X. et al. (2003), Nutrients and carbon budgets for the Gulf of Lion during the Moogli cruises, *Oceanol. Acta*, *26*(4), 421–433, doi:10.1016/S0399-1784(03)00024-0.

Egleston, E. S., C. L. Sabine, and F. M. M. Morel (2010), Revelle revisited: Buffer factors that quantify the response of ocean chemistry to changes in DIC and alkalinity, *Global Biogeochem. Cycles*, *24*, GB1002, doi:10.1029/2008GB003407.

Feely, R. A., C. L. Sabine, J. M. Hernandez-Ayon, D. Ianson, and B. Hales (2008), Evidence for upwelling of corrosive "acidified" water onto the continental shelf, *Science*, *320*(5882), 1490–1492, doi:10.1126/science.1155676.

Garbe, C. S. et al. (2014), Transfer Across the Air-Sea Interface, in *Ocean-Atmosphere Interactions of Gases and Particles*, edited by P. S. Liss and M. T. Johnson, pp. 55–112, Springer Berlin Heidelberg, Berlin, Heidelberg.

Gazeau, F., S. V. Smith, B. Gentili, M. Frankignoulle, and J.-P. Gattuso (2004), The European coastal zone: characterization and first assessment of ecosystem metabolism, *Estuar. Coast. Shelf Sci.*, *60*(4), 673–694, doi:10.1016/j.ecss.2004.03.007.

Hassellöv, I.-M., D. R. Turner, A. Lauer, and J. J. Corbett (2013), Shipping contributes to ocean acidification, *Geophys. Res. Lett.*, *40*, doi:10.1002/grl.50521.

Hofmann, A. F., K. Soetaert, J. J. Middelburg, and F. J. R. Meysman (2010a), AquaEnv : An aquatic acid–base modelling environment in R, *Aquat. Geochemistry*, *16*(4), 507–546, doi:10.1007/s10498-009-9084-1.

Hofmann, A. F., J. J. Middelburg, K. Soetaert, D. A. Wolf-Gladrow, and F. J. R. Meysman (2010b), Proton cycling, buffering, and reaction stoichiometry in

natural waters, *Mar. Chem.*, *121*(1-4), 246–255, doi:10.1016/j.marchem.2010.05.004.

Hunter, K. A. et al. (2011), Impacts of anthropogenic SO_x, NO_x and NH_3 on acidification of coastal waters and shipping lanes, *Geophys. Res. Lett.*, *38*, L13602, doi:10.1029/2011GL047720.

Liss, P. S., and L. Merlivat (1986), Air-sea gas exchange rates: introduction and synthesis, in *The Role of Air-Sea Exchange in Geochemical Cycling*, vol. 185, edited by P. Buat-Ménard, pp. 113–127, Springer Netherlands.

Mehrbach, C., C. H. Culberson, J. E. Hawley, and R. M. Pytkowicz (1973), Measurement of the apparent dissociation constants of carbonic acid in seawater at atmospheric pressure, *Limnol. Oceanogr.*, *18*(6), 897–907, doi:10.4319/lo.1973.18.6.0897.

Meinshausen, M. et al. (2011), The RCP greenhouse gas concentrations and their extensions from 1765 to 2300, *Clim. Change*, *109*(1-2), 213–241, doi:10.1007/s10584-011-0156-z.

Middelburg, J. J., and K. Soetaert (2004), The role of sediments in shelf ecosystem dynamics, in *The Sea*, vol. 13, pp. 353–373.

Midorikawa, T., H. Y. Inoue, M. Ishii, D. Sasano, N. Kosugi, G. Hashida, S. Nakaoka, and T. Suzuki (2012), Decreasing pH trend estimated from 35-year time series of carbonate parameters in the Pacific sector of the Southern Ocean in summer, *Deep Sea Res. Part I Oceanogr. Res. Pap.*, *61*, 131–139, doi:10.1016/j.dsr.2011.12.003.

Orr, J. C. et al. (2005), Anthropogenic ocean acidification over the twenty-first century and its impact on calcifying organisms, *Nature*, *437*(7059), 681–686, doi:10.1038/nature04095.

Provoost, P., S. van Heuven, K. Soetaert, R. W. P. M. Laane, and J. J. Middelburg (2010), Seasonal and long-term changes in pH in the Dutch coastal zone, *Biogeosciences*, *7*(11), 3869–3878, doi:10.5194/bg-7-3869-2010.

Rodhe, H., F. Dentener, and M. Schulz (2002), The global distribution of acidifying wet deposition, *Environ. Sci. Technol.*, *36*(20), 4382–4388, doi:10.1021/es020057g.

Santana-Casiano, J. M., M. González-Dávila, M.-J. Rueda, O. Llinás, and E.-F. González-Dávila (2007), The interannual variability of oceanic CO_2 parameters in the northeast Atlantic subtropical gyre at the ESTOC site, *Global Biogeochem. Cycles*, *21*, GB1015, doi:10.1029/2006GB002788.

Schindler, D. W. (1988), Effects of acid rain on freshwater ecosystems, *Science*, *239*(4836), 149–57, doi:10.1126/science.239.4836.149.

Takahashi, T. et al. (2009), Climatological mean and decadal change in surface ocean pCO_2, and net sea–air CO_2 flux over the global oceans, *Deep Sea Res. Part II Top. Stud. Oceanogr.*, *56*(8-10), 554–577, doi:10.1016/j.dsr2.2008.12.009.

Thomas, H., Y. Bozec, K. Elkalay, and H. J. W. de Baar (2004), Enhanced open ocean storage of CO_2 from shelf sea pumping, *Science*, *304*(5673), 1005–1008, doi:10.1126/science.1095491.

Thomas, H., L. Schiettecatte, K. Suykens, Y. Koné, E. Shadwick, A. Prowe, Y. Bozec, H. de Baar, and A. Borges (2009), Enhanced ocean carbon storage from anaerobic alkalinity generation in coastal sediments, *Biogeosciences*, *6*, 267–274, doi:10.5194/bg-6-267-2009.

Thomas, H., J. Pempkowiak, F. Wulff, and K. Nagel (2010), Carbon and nutrient budgets of the Baltic Sea, in *Carbon and nutrient fluxes in global continental*

margins, edited by K.-K. Liu, L. Atkinson, R. Quinones, and L. Talaue-McManus, pp. 334–346, Springer-Verlag, Germany.

Tsyro, S., and E. Berge (1997), *The contribution of ship emissions from the North Sea and the north-eastern Atlantic Ocean to acidification in Europe*, Oslo.

Wootton, J. T., and C. A. Pfister (2012), Carbon system measurements and potential climatic drivers at a site of rapidly declining ocean pH, *PLoS One*, *7*(12), e53396, doi:10.1371/journal.pone.0053396.

Yool, A., A. P. Martin, C. Fernández, and D. R. Clark (2007), The significance of nitrification for oceanic new production, *Nature*, *447*(7147), 999–1002, doi:10.1038/nature05885.

Zhai, W., M. Dai, W.-J. Cai, Y. Wang, and H. Hong (2005), The partial pressure of carbon dioxide and air–sea fluxes in the northern South China Sea in spring, summer and autumn, *Mar. Chem.*, *96*(1-2), 87–97, doi:10.1016/j.marchem.2004.12.002.

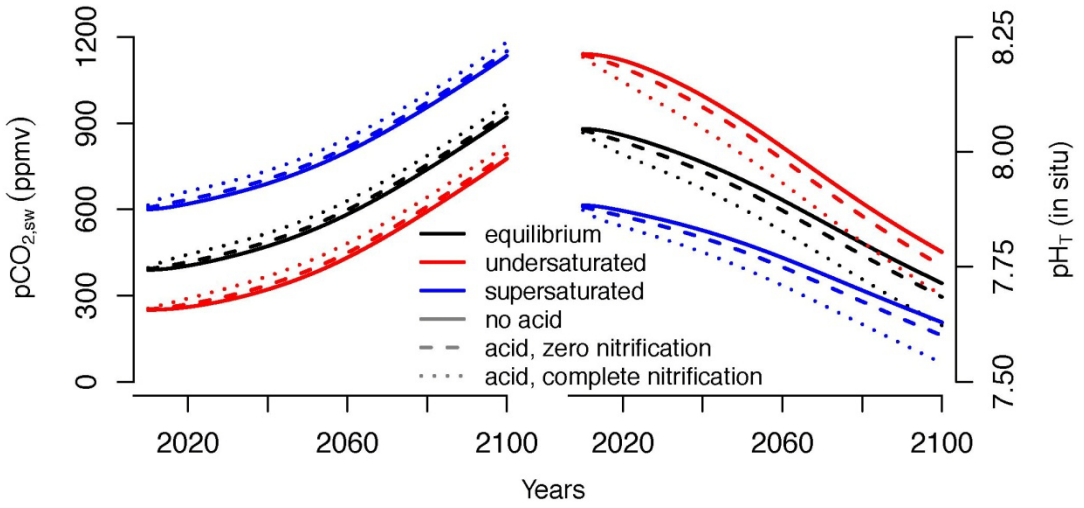

Figure 1: Different effects of atmospheric deposition and $pCO_{2,atm}$ increase on a supersaturated and an undersaturated system. Initial conditions: TA = 2260 µmol kg^{-1}, S=34, T=12°C, $pCO_{2,sw}$ = 389 ppmv (equilibrated system), 250 ppmv (undersaturated system) or 600 ppmv (supersaturated system). The increase in $pCO_{2,atm}$ was taken from the RCP8.5 scenario. Acid deposition leads to a decrease in TA of 1.34 (no nitrification) or 3.94 µmol kg^{-1} yr^{-1} (complete nitrification). pH on total scale, equilibrium constants of *Mehrbach et al.* [1973] as refitted by *Dickson and Millero* [1987].

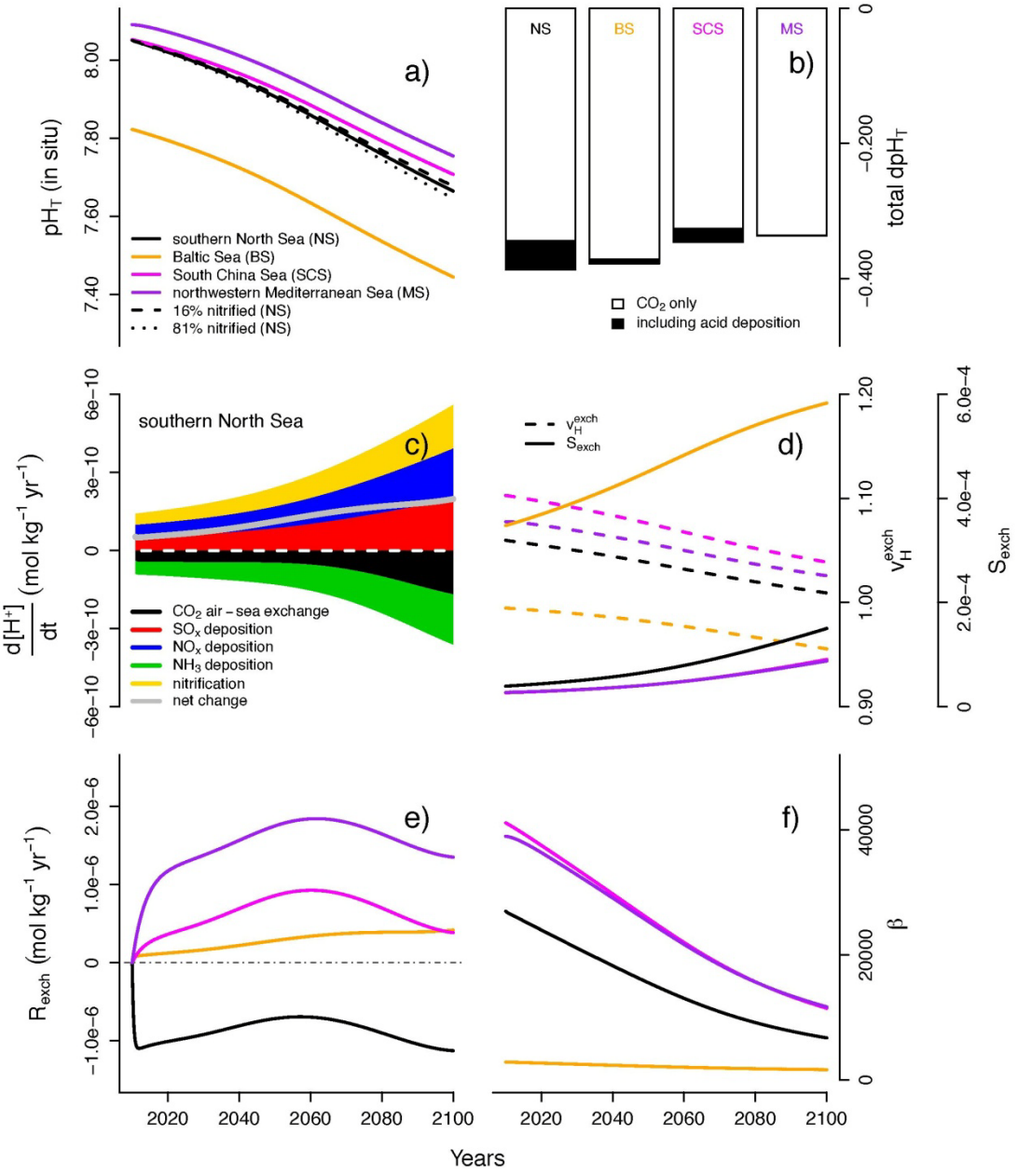

Figure 2: Model output for the four different coastal seas using a constant acid deposition flux, 43% nitrification of NH_3 input and the RCP8.5 scenario for $pCO_{2,atm}$. a) pH_T at *in situ* temperature; b) total ΔpH_T without and with acid deposition; c) contribution of separate processes to net $[H^+]$ change in southern North Sea; d) sensitivity (S_{exch}) and stoichiometric proton coefficient (ν_H^{exch}) of CO_2 air-sea exchange; e) uncorrected contribution of CO_2 air-sea exchange to proton balance (R_{exch}); f) buffering capacity.